Journal of Thermal Analysis and Calorimetry, Vol. 91 (2008) 2, 641–647

PYROLYSIS OF PISTACHIO SHELL AS A BIOMASS

*Y. Tonbul**

Dicle University, Faculty of Science and Art, Department of Chemistry, 21280 Diyarbakir, Turkey

There is an increasing concern with the environmental problems associated with the increasing CO_2, NO_x and SO_x emissions resulting from the rising use of fossil fuels. Renewable energy, mainly biomass, can contribute to reduce the fossil fuels consumption. Biomass is a renewable resource with a widespread world distribution. Pistachio is available in large quantities in Gaziantep region in Turkey. Pistachio shell has a good energy potential for exploitation through pyrolysis and gasification.

This study deals with the thermal degradation characteristics of in different particle sizes pistachio shell and its kinetics. Thermal degradation analysis have been done by using a thermogravimetric analyzer from room temperature to 800°C in N_2 atmosphere at different heating rates (5, 10, 15 and 20°C min^{-1}). TG and DTG curves exhibited two distinct degradation zones. Kinetic parameters were calculated by using Coats–Redfern method and model-free isoconversional Flynn–Wall–Ozawa (FWO) kinetic method.

Keywords: *Coats–Redfern method, FWO method, pistachio shell, pyrolysis, thermogravimetry*

Introduction

Biomass can generally be defined as any hydrocarbon material which mainly consists of carbon, hydrogen, oxygen and nitrogen. Sulfur is also present in less proportion. Some biomass types also carry significant proportions of inorganic species. The concentration of the ash arising from these organics changes from less than 1% in softwoods to 15% in herbaceous biomass and agricultural residues [1]. Another definition is that every type of combustible substances except fossil fuels is described as biomass. Municipal solid wastes, agricultural and forest solid wastes, and aquatics are some of the well-known classes of biomass [2].

Nowadays there is a great concern with the environmental problems associated with the great CO_2, NO_x and SO_x emissions resulting from the rising use of fossil fuels. For this reason, more attention is being paid to renewable energy, especially biomass energy. In order to mitigate the greenhouse effect on the climatic change the EU has elaborated the 2003/87/CE Directive, in which the CO_2 emission quota for each Union European country is fixed. The new technologies must allow fulfilling the objective of the CO_2 emission reduction by saving energy, diversifying the energy sources and making the energy-production processes more efficient. The renewable energy, especially biomass energy, will pay an important role in this goal. According to EU objectives, 22.1% of electricity should be generated from renewable energy [3].

The thermolytic behavior of biomass materials primarily depends on its chemical composition and structure. The degree of crystallinity and polymerization of the starting materials are integral in defining their respective thermal degradation behavior. In addition to the above parameters, experimentally derived kinetic parameters also depend on the specific pyrolysis condiions that include temperature, heating rate, pressure, particle size and ambient gas environment [4].

The major organic components of biomass can be classified as cellulose, hemicellulose and lignin. Cellulose is a polysaccharide and forms the skeletal structure of most terrestrial biomass and constitutes approximately 50% of the cell wall material. Hemicellulose is a complex polysaccharide takes place in association with cellulose in the cell wall, but unlike cellulose, hemicelluloses are soluble in dilute alkali and consists of branched structures, which vary considerably among different woody and herbaceous biomass species. The lignin is highly branched, substituted, mononuclear aromatic polymers in the cell walls of certain biomass, especially woody species, and more often bound to adjacent cellulose fibers to form a lignocellulosic complex [1].

When the biomass is burned, the released carbon goes back to the atmosphere and will be recycled into the next generation of growing plants. Therefore, the application of biomass for energy can lead to zero net CO_2 emission in a very short life cycle periods, since carbon in the form of CO_2 and energy are fixed by photosynthesis during biomass growth. On the other hand, most of biomass residues can represent an important environmental problem when stored or land filled without control because it undergoes anaerobic fermentation, resulting in the formation of methane. This compound has absorption capacity of the infra-

* ytonbul@dicle.edu.tr

1388–6150/$20.00

Akadémiai Kiadó, Budapest, Hungary
Springer, Dordrecht, The Netherlands

red radiation 23 times higher than CO_2, thus its incidence on greenhouse effect is very high. Moreover, methane affects also the formation of tropospheric (ground-level) ozone, which can affect human health, vegetation, and building materials. Thus the use of biomass residues as energy source has a double positive effect from an environmental viewpoint [3].

Pistachio is the one of the most common agricultural product of Turkey and world. According to the Foreign Agriculture Service of the United States Department of Agriculture, the world pistachio production was 0.21 million tonnes in 1999. This will then result in large quantities of shells being generated [4]. On the other hand, according to Agriculture Ministry of Turkey, annual pistachio production of Turkey is varied from $3 \cdot 10^4$ to $9 \cdot 10^4$ tonnes.

Due to high variety of raw material, the processes that lead to direct energy, combustibles and chemicals from biomass transformation are numerous. A good solution for technical application of biomass energy is conversion of biomass by pyrolysis, gasification or combustion processes. Kinetic data of a pyrolysis reaction is useful for the monitoring and improving efficiency of commercial pyrolyser, gasifier and combustor.

Particularly thermal analysis, thermogravimetry (TG), derivative thermogravimetry (DTG), differential thermal analysis (DTA), differential scanning calorimetry (DSC), seem to be useful for the characterization of the compost organic matter, because of their rapid determination and simplicity as well [5, 6]. In recent years the application of TG, DSC and DTG to study the combustion and pyrolysis behavior of fossil fuels and their derivatives has gained a wide acceptance among researchers, which is of exceptional significance for industry and for the economy [7–11].

In this study, the effect of particle size on the pyrolysis kinetic parameters of pistachio shell were aimed.

Experimental

Pistachio shell from Gaziantep region of Turkey was used in this study. After drying in an oven at 105°C the samples were crushed by a jaw breaker (Retsch BB 1/A) and ground in a rotor beater mill (Retsch SRZ).

Sieve analysis (passing a known amount of the sample material successively through a series of standard sieves of decreasing size) is one of the oldest methods to determine size distribution of solid particles. The Retsch 3B model test-sieving machine (Tyler series sieves: 3360–71 μm) was used, and the grain-size classes were weighed an analytical balance.

Elemental analysis of the samples were done by Carlo Erba model 1108 elemental analyzer calibrated with standard compounds using the K factor calculation.

The pyrolysis experiments were carried out by non-isothermal thermogravimetry using Shimadzu TGA-50 analyzer. Thermal gravimetric experimental procedure involves placing the sample (max. amount 20 mg) into a platinum crucible and then heating ambient to 800°C at different linear heating rates of 5, 10, 15 and 20°C min^{-1} and with a nitrogen flow rate of 30 mL min^{-1}. The mass losses occurring in correspondence to the temperature rises were continuously recorded with a computer working in coordination with the furnace and the control unit of the analyzer, in order to collect the data required to determine the pyrolysis characteristics and kinetics of the samples.

Results and discussion

Table 1 shows the ultimate analysis and proximate analysis results according to particle size.

It is seen from the table that there is no S. This is interesting from environmental and technical point of view because some S derivatives are important atmospheric contaminants and negatively affect the installation. SO_2 emissions result in acid rain, causing health, environmental and material damages, and it is transformed in the atmosphere to small particles that can have a very long life-time. The high volatile matter found in the samples suggests the high potential of this residue for energy production by pyrolysis and gasification [3].

Typical TG and DTG curves of pistachio shell particle size –0.125+0.071 mm obtained from 5°C min^{-1} are presented in Fig. 1.

It is generally recognized that the pyrolysis of biomass involves various individual peaks or shoulders on the DTG curve, taking place from decomposition of the

Table 1 Ultimate and proximate analysis of pistachio nut shell

Sample size/mm	Ultimate analysis/%			Proximate analysis/%		
	C	H	O	moisture	VM	ash
–0.60+0.250	46.76	5.28	47.96	3.59	88.22	0.61
–0.25+0.125	47.13	5.24	47.63	3.12	91.48	0.66
–0.125+0.071	47.55	5.48	46.97	3.34	95.16	0.99

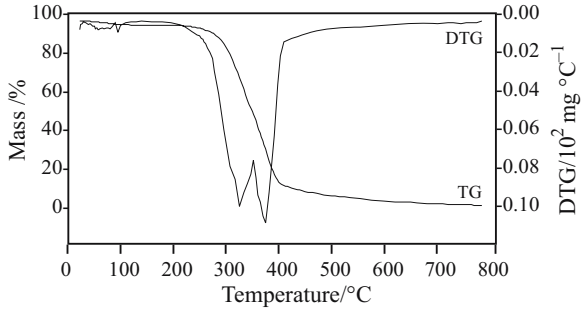

Fig. 1 TG and DTG curves of pistachio nut shell particle size –0.125+0.071 mm obtained from 5°C min^{-1}

major components of biomass such as hemicellulose, cellulose and lignin. Hemicellulose and cellulose can be easily decomposed under miscellaneous pyrolysis conditions, since these oxygen rich constituents show high thermal reactivity under decomposing conditions. This is because, some volatiles release after moisture removal as a result of disintegration of hemicelluloses, and just after that cellulose is begun to disintegrate, giving further volatiles as temperature increases. Of the major constituents of biomass, lignin is not as thermally reactive as hemicellulose and cellulose. Although lignin also began to decompose while hemicellulose and cellulose were decomposing, the peaks of hemicellulose and cellulose masked its peaks at lower temperatures. Lignin peaks can be shown on the DTG curves as a tailing section especially at higher temperatures, after completion of the previous peaks of other two components [2].

It is seen from the DTG diagram (Fig. 1) that there are three peaks. First is around 100°C and corresponding to remove of the moisture. Second is beginning around 200°C and finishing 350°C. Between these temperatures, hemicellulose is decomposing and finally, third peak is beginning around 350°C and lasting to 800°C. This peak is corresponding to decomposing of cellulose and lignin. According to particle size and heating rate, these values are presented in Table 2. It is clearly seen from the Table 2 that initial and final decomposing temperatures, temperature of maximum mass loss rate and lost amounts are increase, when heating rates increase. On the other hand, upon particle size increases, all the above values increase.

Compared with isothermal experiments, non-isothermal runs are more convenient to carry out because it is not necessary to perform a sudden temperature jump of the sample at the beginning. However, Arrhenius parameters obtained from non-isothermal are often reported to disagree with the values derived from isothermal experiments [12].

Modelling of a reaction for combustion and pyrolysis processes of natural matter is extremely complicated because several components are oxidized simultaneously. In the present work, data from TG and DTG curves were used to determine the kinetic parameters. Mathematical analysis was performed by integral method of Coats and Redfern kinetic model and Flynn–Wall–Ozawa (FWO) kinetic model.

The methods of kinetics processing can be divided into two main categories: those which employ data obtained under only one heating rate, and those based on performing series of measurements under different heating rates (isoconversional methods). The attraction of isoconversional methods derives mainly from its ability to give activation energy values without the necessity of presuming the analytical form of the conversion model. The basic assumption of model-free isoconversional methods is that the reaction rate at a constant conversion is only a function of temperature, and that the reaction model is not dependent on temperature or heating rate [13].

Table 2 Initial and final mass loss temperatures, and temperatures of maximum mass loss rate of pistachio nut shell at studied pyrolysis conditions for different heating rates and particle sizes

Particle size/mm	Heating rate/°C min^{-1}	Step 1			Step 2		
		T_i/°C	T_f/°C	T_M/°C	T_i/°C	T_f/°C	T_M/°C
–0.600+0.250	5	227.2	324.9	294.3	324.9	800.0	356.7
	10	239.7	337.0	306.2	337.0	800.0	369.1
	15	247.4	345.2	311.7	345.2	800.0	377.9
	20	251.7	350.9	318.7	350.9	800.0	381.3
–0.250+0.125	5	215.2	325.4	298.7	325.4	800.0	353.5
	10	224.4	340.2	312.1	340.2	800.0	365.6
	15	234.8	347.7	318.7	347.7	800.0	371.6
	20	242.6	356.3	326.0	356.3	800.0	379.4
–0.125+0.071	5	200.0	317.3	303.6	317.3	800.0	350.6
	10	215.1	333.7	316.9	333.7	800.0	363.9
	15	225.9	345.8	326.4	345.8	800.0	374.4
	20	233.3	353.4	332.4	353.4	800.0	381.2

T_i – initial temperature, T_f – final temperature, T_M – maximum mass loss rate temperature

Table 3 Activation energies calculated from Coats–Redfern method for different heating rates and particle sizes/kJ mol^{-1}

Particle size/mm	Heating rate/ °C min^{-1}	Step 1					Step 2				
		reaction order					reaction order				
		0.5	2/3	1	1.25	1.50	0.5	2/3	1	1.25	1.50
–0.600+0.250	5	117	124	140	168	168	205	212	226	251	250
	10	122	130	147	176	176	217	225	240	265	264
	15	128	136	154	191	184	220	227	243	268	267
	20	130	138	155	187	186	220	228	243	270	268
	avr.	124	132	149	181	179	216	223	238	264	262
–0.250+0.125	5	107	114	128	153	153	182	189	202	224	223
	10	110	117	130	158	157	204	211	226	251	250
	15	115	122	138	165	164	200	207	222	246	245
	20	115	122	138	165	165	216	223	239	265	264
	avr.	112	119	134	160	160	201	208	222	247	250
–0.125+0.071	5	102	108	122	145	145	170	176	189	209	209
	10	103	109	123	147	146	200	207	221	245	244
	15	104	111	124	148	148	216	224	239	265	264
	20	107	113	127	152	151	225	233	249	276	275
	avr.	104	110	124	148	148	203	210	225	249	248

Table 4 log*A* values calculated from Coats–Redfern method for different heating rates and particle sizes/mg^{1-n} min^{-1}

Particle size/mm	Heating rate/ °C min^{-1}	Step 1					Step 2				
		reaction order					reaction order				
		0.5	2/3	1	1.25	1.50	0.5	2/3	1	1.25	1.50
–0.600+0.250	5	10.28	11.06	12.30	15.53	15.49	16.83	17.46	18.35	20.89	20.79
	10	10.87	11.66	12.95	16.26	16.22	17.83	18.48	19.41	22.02	21.91
	15	11.46	12.27	13.62	17.02	16.98	17.96	18.61	19.54	22.14	22.04
	20	11.59	12.40	13.74	17.13	17.09	17.99	18.64	19.58	22.19	22.09
	avr.	11.04	11.85	13.15	16.49	16.45	17.65	18.30	19.22	21.81	21.71
–0.250+0.125	5	9.29	10.00	11.09	14.07	14.03	14.86	15.45	16.24	18.62	18.53
	10	9.62	10.33	11.44	14.44	14.40	16.69	17.33	18.23	20.76	20.67
	15	10.14	10.87	12.01	15.08	15.04	16.29	16.91	17.78	20.27	20.19
	20	10.12	10.85	11.99	15.06	15.02	17.53	18.19	19.14	21.76	21.67
	avr.	9.79	10.51	11.63	14.66	14.62	16.34	16.97	17.85	20.35	20.27
–0.125+0.071	5	8.90	9.57	10.59	13.42	13.38	13.94	14.50	15.24	17.52	17.45
	10	9.03	9.69	10.70	13.51	13.48	16.47	17.09	17.96	20.45	20.36
	15	9.10	9.77	10.77	13.58	13.54	17.74	18.40	19.34	21.96	21.86
	20	9.37	10.04	11.05	13.87	13.84	18.45	19.12	20.11	22.80	22.70
	avr.	9.10	9.77	10.78	13.60	13.56	16.65	17.28	18.16	20.68	20.59

Coats and Redfern kinetic model has been successfully used for studies on the kinetics of decomposition of solid substances [14–18].

The calculation of the kinetic data is based on the formal kinetic equation

$$\left[\frac{\mathrm{d}\alpha}{\mathrm{d}t}\right]=k\alpha^{n} \quad (1)$$

where α is the amount of sample undergoing the reaction, n is the order of reaction and k is the specific rate constant.

Coats and Redfern developed an integral method, which can be applied to thermogravimetric data, assuming the order of reactions. The correct order is presumed to lead to the best linear plot, from which the activation energy is determined. The final form of the equation, which is used for the analysis, takes the form

$$\log\left[\frac{1-(1-\alpha)^{1-n}}{T^2(1-n)}\right]=\log\frac{AR}{\beta E}\left[1-\frac{2RT}{E}\right]-\frac{E}{2.303RT} \quad \text{for } n\neq 1 \quad (2)$$

$$\log\left[\frac{-\log(1-\alpha)}{T^2}\right]=\log\frac{AR}{\beta E}\left[1-\frac{2RT}{E}\right]-\frac{E}{2.303RT} \quad \text{for } n=1 \quad (3)$$

where β is the heating rate (K min^{-1}).

By plotting the appropriate left-hand side of the equations *vs.* $1/T$, the slope equals $-E/2.303R$. The activation energy (E), Arrhenius constant (A) and reaction rate constant (k) can be calculated from these equations [15]. An integral method, which can be applied to TG/DTG data assuming the order of reactions, was also applied. The correct order is presumed to lead to the best linear plot, from which the activation energy is determined.

The isoconversional method of Flynn, Wall and Ozawa is a model-free method which involves measuring the temperatures corresponding to fixed values of α (conversion degree) from experiments at different rates, β, and plotting $\ln\beta$ *vs.* $1/T$

$$\ln\beta=\ln\left[A\frac{f(\alpha)}{(\mathrm{d}\alpha/\mathrm{d}t)}\right]-\frac{E_a}{RT} \quad (4)$$

and the slopes of such plots give $-E_a/R$. If E_a varies with α, the results should be interpreted in terms of multi-step reaction mechanism [12].

To determine the kinetic parameters, according to Coats–Redfern method, different reaction orders (0.5, 2/3, 1, 1.25 and 1.5) were assumed and data analysed according to Eqs (2) and (3). The reaction order was ascertained on the basis of best-fit criteria between experimental and predicted results. Results of Coats–Redfern and FWO calculations are presented in Tables 3–6, respectively. For step 2, activation energy values were calculated in the range of $0.1\leq\alpha\leq 0.6$, because out of that range, reaction order was diverged from assumed order.

In the step 1, best correlation coefficients (>0.99) were obtained from Mampel (first order) reaction model [12]. On the other hand, it also suggested that step 2 obey power law reaction model, and that was corresponding to 3/2nd reaction order.

For the step 1, correlation between activation energy values calculated from Coats–Redfern method and FWO method are compatible each other. But, for the step 2, this expression is not true. This was mainly due to, in Coats–Redfern calculations, upon heating rate increases, initial and final decomposing tempera-

Table 5 Activation energies calculated from FWO method for different particle sizes/kJ mol^{-1}

Particle size/mm		Conversion degree/%									
		10	20	30	40	50	60	70	80	90	Avr.
–0.600+0.250	Step 1	138	143	148	147	160	164	168	169	166	156
	Step 2	173	176	181	186	185	187	–	–	–	181
–0.250+0.125	Step 1	129	133	138	143	147	150	151	151	147	143
	Step 2	150	157	165	171	174	176	–	–	–	166
–0.125+0.071	Step 1	115	119	121	123	123	123	125	123	124	122
	Step 2	130	133	140	148	157	165	–	–	–	146

Table 6 log$A$ values calculated from FWO method for different particle sizes/mg^{1-n} min^{-1}

Particle size/mm		Conversion degree/%									
		10	20	30	40	50	60	70	80	90	Avr.
–0.600+0.250	Step 1	12.14	12.29	12.58	12.22	13.18	13.34	13.35	13.12	12.43	12.74
	Step 2	13.98	13.82	13.97	14.16	13.93	13.94	–	–	–	13.97
–0.250+0.125	Step 1	11.39	11.45	11.64	11.88	12.00	12.02	11.86	11.50	10.71	11.60
	Step 2	12.01	12.32	12.76	13.05	13.10	13.07	–	–	–	12.72
–0.125+0.071	Step 1	10.20	10.21	10.18	10.17	9.95	9.78	9.69	9.26	8.93	9.82
	Step 2	10.47	10.42	10.81	11.29	11.86	12.32	–	–	–	11.19

tures increase. This was lead to reduce temperature range of step 2 and finally, kinetic parameters calculated by using Coats–Redfern method were higher than by using FWO method.

Conclusions

Pistachio shell samples have been analysed by thermogravimetry due to great potential of this biomass for energy uses. TG analysis was made from room temperature up to 800°C at different heating rates: 5, 10, 15 and 20°C min^{-1}. Results showed three degradation regions. First was due to dehydration of samples about 100°C. Second and third one (about 200 and 320°C) was corresponding to degradation of hemicellulose and cellulose. Then kinetic parameters of samples were calculated using Coats–Redfern method and FWO method.

For degradation of hemicellulose region (step 1), reaction was fitted to Mampel (first order) reaction model and activation energy and log*A* values were varied from 124 to 149 kJ mol^{-1}, and from 10.78 to 13.15 mg^{1-n} min^{-1}, respectively, using Coats–Redfern method and varied from 122 to 156 kJ mol^{-1}, from 9.82 to 12.74 mg^{1-n} min^{-1}, respectively, using FWO method. It is from the results that, there is seen a good correlation between two methods.

For degradation of cellulose region (step 2), reaction was fitted to power law reaction model and activation energy and log*A* values were varied from 248 to 262 kJ mol^{-1}, and from 20.59 to 21.71 mg^{1-n} min^{-1}, respectively, using Coats–Redfern method and varied from 146 to 181 kJ mol^{-1}, and from 11.19 to 13.97 mg^{1-n} min^{-1}, respectively, using FWO method.

Acknowledgements

The author thanks Canan KAYA for carrying out ultimate and proximate analysis on the samples.

References

1 S. Yaman, Energ. Convers. Manage., 45 (2004) 651.
2 H. H. Acma, J. Anal. Appl. Pyrolysis, 75 (2005) 211.
3 V. Mangut, E. Sabio, J. Ganan, J. F. Gonzalez, A. Ramiro, C. M. Gonzalez, S. Roman and A. Al-Kassir, Fuel. Process. Technol., 87 (2006) 109.
4 T. Fisher, M. Hajaligol, B. Waymack and D. Kellog, J. Anal. Appl. Pyrolysis, 62 (2002) 331.
5 M. Pietro and C. Paola, Thermochim. Acta, 413 (2004) 209.
6 J. Peuravuori, N. Paaso and K. Pijlaha, Thermochim. Acta, 361 (1999) 181.
7 M. V. Kök and M. R. Pamir, J. Anal. Appl. Pyrolysis, 35 (1995) 145.
8 G. Steiner, J. Rath, M. G. Wolfinger and G. Staudinger, Thermochim. Acta, 398 (2003) 59.
9 M. V. Kök, G. Pokol, C. Keskin, J. Madarász and S. Bagci, J. Therm. Anal. Cal., 76 (2004) 247.
10 M. V. Kök, J. Therm. Anal. Cal., 64 (2001) 1319.
11 J. M. Nazzal, J. Therm. Anal. Cal., 65 (2001) 847.
12 S. Vyazovkin and C. A. Wight, Thermochim. Acta, 340 (1999) 53.
13 R. Lopez-Fonseca, I. Landa, M. A. Guiterrez-Ortiz and J. R. Gonzalez-Velasco, J. Therm. Anal. Cal., 80 (2005) 65.
14 M. A. Olivella and F. X. C. de la Heras, Thermochim. Acta, 385 (2002) 171.
15 Y. Tonbul and K. Yurdakoc, Turk. J. Chem., 25 (2001) 333.
16 M. V. Kök, Energ. Source, 25 (2003) 1007.
17 M. Z. Duz, Y. Tonbul, A. Baysal, O. Akba, A. Saydut and C. Hamamci, J. Therm. Anal. Cal., 81 (2005) 395.
18 Y. Tonbul, A. Saydut and C. Hamamci, Oil Shale, 23 (2006) 286.

Received: March 5, 2007
Accepted: May 22, 2007
OnlineFirst: October 13, 2007

DOI: 10.1007/s10973-007-8428-6